A GAUSSIAN MODEL TO INVESTIGATE THE PHOTOLUMINESCENCE SPECTRA OF NANOPOROUS SILICON QUANTUM WIRES

SUBMITTED IN PARTIAL FULFILLMENT OF THE
REQUIREMENTS FOR THE DEGREE OF
MASTER OF SCIENCE IN PHYSICS
AT
ADDIS ABABA UNIVERSITY
ADDIS ABABA, ETHIOPIA
JUNE 2009

By

Zebib yenus

zebibnate@yahoo.com

ADDIS ABABA UNIVERSITY
DEPARTMENT OF
PHYSICS

The undersigned hereby certify that they have read and recommend to the School of Graduate Studies for acceptance a thesis entitled "***A GAUSSIAN MODEL TO INVESTIGATE THE PHOTOLUMINESCENCE SPECTRA OF NANOPOROUS SILICON QUANTUM WIRES***" by **Zebib yenus** in partial fulfillment of the requirements for the degree of **Master of Science in Physics**.

Dated: June 2009

Supervisor: _____
Dr. Sib Krishna Ghoshal

Examiners: _____
Dr. Gizaw Mengistu

_____
Prof. A. V. Gholap

ADDIS ABABA UNIVERSITY

Date: **June 2009**

Author: **Zebib yenus**

Title: ***A GAUSSIAN MODEL TO INVESTIGATE THE PHOTOLUMINESCENCE SPECTRA OF NANOPOROUS SILICON QUANTUM WIRES***

Department: **Physics**

Degree: **M.Sc.** Convocation: **June** Year: **2009**

Permission is herewith granted to Addis Ababa University to circulate and to have copied for non-commercial purposes, at its discretion, the above title upon the request of individuals or institutions.

Signature of Author

For commemoration to my pleasant, self-starter and genuine father **Yenus Nuru** *(10 November 2008,)*

Table of Contents

List of Figures

Abstract

The observation of visible luminescence with finite quantum efficiency at room temperature from nanoporous silicon (nP-Si) prompted renewed hope for the possible integration of Silicon (Si) based light emitting devices. Since then, nP-Si quantum wires research has attracted considerable attention. However, the origin of photoluminescence (PL) and the blue shift in PL peak is still a debatable issue.

We present a phenomenological model formulation to explain PL spectra from np-Si with diameters of wires ranging from 1-6 nm based on the quantum confinement model. We explicitly calculate the expression for PL spectra as a function of energy upshift. And we take the size distribution of nanoporous Si quantum wires as Gaussian. To validate our model we compare our simulated PL spectra with experiments. To observe the nature of blue shift further we use the energy gap vs. diameter as an input parameter from pseudopotential simulation and tight binding fit to our model and generate PL that shows the same nature as experimental one. Our results clearly show the blue shift of PL as a function of energy upshift and wavelength by varying the diameter of wires. We believe that Gaussian model looking at PL of nP-Si quantum wires is new observation that provide very good qualitative agreement with other observations.

Acknowledgements

First and foremost, I would like to thank my advisor Dr. Sib Krishna Ghoshal, who has given support during this research. His limitless and invaluable effort in guiding, advising and providing the supportive materials for the accomplishment of this thesis gives me a great pleasure. Especially, I highly praise him for letting me start my works earlier. His teaching experience has contributed immensely to the successful completion of my studies.

I would like to thank my family and friends who have been great source of hope and inspiration. Above all, I would like to express my heartfelt gratitude to my husband for all the love, support, understanding and encouragement he provided.

Addis Ababa,Ethiopia

Zebib Yenus

Chapter 1

Introduction

In this chapter we are going to discuss what Si nanostructures are, and how are they fabricated, and also how the density of states changes as one goes from bulk (3-D) dimension structure to lower (0-D) dimension. Finally we will discuss how the band gap of nanostructures gets affected by the quantum confinement effect.

The general objective of the thesis is to investigate the expression for PL spectra as a function of energy upshift to formulate Gaussian line shape and to show how PL spectra shifts for different mean diameters of nanoporous silicon quantum wires.

The specific objectives of the thesis are:

- To calculate PL spectra expression as a function of energy upshift.
- To investigate the size distribution of nanoporous column as Gaussian.
- To show how the PL peak shifts with mean diameter of Si quantum wire; and
- To validate our model with other theoretical and experimental findings.

1.1 Si nanostructures

Nanoscience and nanotechnology pertain to the synthesis, characterization, exploration, interrogation, exploitation, and utilization of nanostructured materials, which are characterized by at least one dimension in the nanometer range. Such nanostructured systems constitute a bridge between single molecules and infinite bulk systems. Individual nanostructures involve clusters, nanoparticles, nanocrystals, quantum dots, nanowires, and nanotubes, while collections of nanostructures involve arrays, assemblies, and superlattices of individual nanostructures. The chemical and physical properties of nonmaterial can significantly differ from those of bulk materials of the same chemical composition. The uniqueness of the structural characteristics, energetic, response, dynamics, and chemistry of nanostructures is novel and constitutes the experimental and conceptual background for the novel field of nanoscience. Suitable control of the properties and response of nanostructures can lead to new devices and technologies [1].

For example pure Si is the most widely used material for optoelectronic applications since many years and its fabrication technology is highly developed. However, the indirect band gap of bulk Si presents a problem for light-emitting applications. A solution that has been proposed to circumvent this problem is nanostructurization of Si in structures comprising porous,Si nanocrystals has stirred research interest in the area of Si nanostructures as a potential candidate for silicon based light emission devices [2].

Therefore Low dimensional silicon is a fascinating material which still has many unfold properties. The main motivation to study silicon comes from its success and

dominance in modern technology, especially in optoelectronics. Indeed nanometer sized transistors are now switching in computers at working frequency exceedingly few GHz. Convergence between microelectronics and telecommunications is looked for in order to couple the computing power of microprocessor with the transmission power of optical fibers. In this effort, merging of various semiconductor technologies is attempted in order to improve on one side the optical properties of microelectronic materials and, on the other side, to reduce the cost of photonic devices. With this respect silicon photonics is playing a key role [3].

Thus we can say reducing any piece of material from a shank to the nanometer scale using different approaches changes virtually all of its most basic properties in a fundamental way. So due to quantum confinement effect, Material different properties change gradually as one goes from bulk to nano region that accompanied different applications such as micro- and optoelectronics, sensors and a biomedical application.

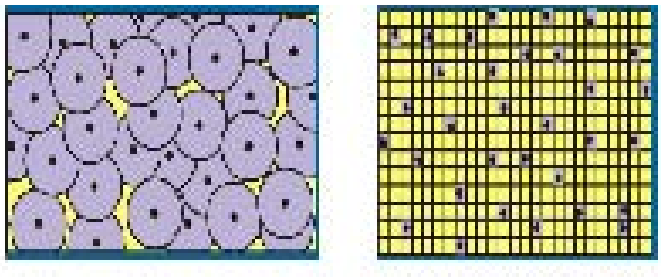

Figure 1.1: Bulk Si (left) and Si nanostructure (right) ([1]).

1.1.1 Fabrication of nanostructures

There are two approaches to build nanostructures with various degrees of quality, speed and cost both having their origins in the semiconductor industry. These are "bottom-up" and "top-down" approaches. The possibility of combining the two approaches opens up new nanomanufacture capabilities [4].

Top-down approach involves a larger material such as a silicon wafer, photonic crystal devices is processed by removing matter until only the nanoscale features remain. Unfortunately, these techniques require the use of lithography.

The traditional bottom-up approach starts with constituent materials and uses chemical, electrical, or physical forces to build a nonmaterial atom-by-atom or molecule-by-molecule. Most nanostructure semiconductors like Si with high hardness values are created with this approach as shown in Fig.1.2 [5].

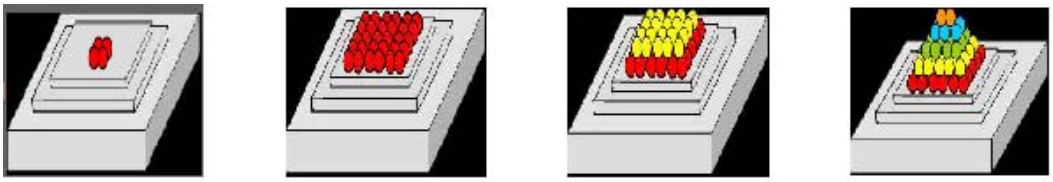

Figure 1.2: Si nanostructure grow continuously from smaller vertically layer- by-layer to large grid [5].

For instance depending on the sizes of pore diameter, p-Si is classified as nanoporous (pore size less than 5 nm), meso-porous (pore size 5-50 nm), and micro-porous (greater than 50 nm) as shown in Fig.1.3 [6].

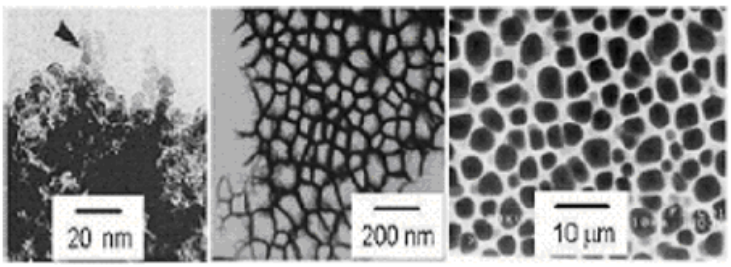

Figure 1.3: Different p-Si structures: nanoporous (left), meso-porous (middle) and macro- porous (right)[6].

Thus the combination of the two approaches leads to new hybrid methods of manufacturing nanostructures. And the bottom up approach is a method of choice for creating large grids of quantum dots and quantum wires.

1.1.2 Applications of Si nanostructure

Low-dimensional semiconductor structures are of high interest due to the significant technological implications in optics and nanoelectronics. The wide interest in nanosolid or porous silicon (P-Si) resulted primarily from the proposal in 1990, that states efficient visible light emission from high porosity structures. However, nanoscale silicon is a complex material with regard to its stability, because its optical properties show environmental and ageing degradation with resulting ambiguity in device performance evaluation.

Silicon nanostructures have tremendous applications in optoelectronic, emission of light and photonic devices. They can be easily integrated into silicon wafer processing and utilized for biological and chemical sensing, potential applications in silicon-based optoelectronic integrated circuits or for light-emitting devices, optical sensors, photo sensors, catalysts and memory devices. Silicon nanostructures can be used for optical

communication technology to develop photonic integrated circuits: optical chips in which optical signals are guided, split, switched, multiplexed or amplified [7].

1.2 Effect of quantum confinement on nanosizing

One of the most direct effects of reducing the size of materials to the nanometer range is the appearance of quantization effects due to the confinement of the movement of electrons, this leads to discrete energy levels depending on the size of the structure. Following this line artificial or natural structure with properties different from those of the corresponding bulk materials can be created. Control over dimensions as well as composition of structures makes it possible to tailor material properties to specific applications which is influenced by quantum confinement effect (QCE)[7].

Hence Quantum confinement (QC) in semiconductors results from the geometric confinement of electrons, holes or excitons (electron hole bound pair). The normal size of an exciton in a large bulk crystal is expressed as an exciton bohr radius (BER). When an electron-hole pair is squeezed below the dimensions approaching exciton bohr radius, quantum confinement effects become prominent in the structure and the effective band gap increases. The smaller the nanostructure the larger the effective band gap and the greater the energy of optical emission which changes the optical and electronic properties when the sample size is sufficently smaller than 10 nm. This effect can also be understood from Heisenbergs uncertainty principle according to which energies of an electron or hole increase as their position is confined.

As a result the effect of QC is a rearrangement of the density of electronic states in energy as direct consequence of volume shrinking in one, two, or even three dimensions,

which can be obtained, respectively, in quantum wells, wires, and dots [8].

Thus understanding of the spatial confinement of electrons with in the crystallite boundary leads to a larger spacing between band gap to change various properties and physical structure of the material as the size of the nanostructure decreased.

1.2.1 Effect of quantum confinement on density of states

In semiconductors of finite size, there is pronounced quantum confinement effect (QCE) on the electronic absorption spectra. Moreover, the wave function describing the behavior of electrons and holes and the number of states per unit energy, i.e., the density of states (DOS), changes as a function of the energy of the particle in different directions [9].

So as we confine the nanostructure from bulk to zero dimensions their densities of states depends on the dimension and on the corresponding wave vector. Let's see one by one how the DOS varies in different dimensions and wave vectors as one goes from 3-D to 0-D.

For bulk (3-D) materials the density of states increases with the energy of the particle following parabolic law. Hence for three dimensional bulk materials, the DOS is proportional to $E^{\frac{1}{2}}$ and is given by

$$D(E) = \frac{2^{\frac{1}{2}} m_e^{\frac{3}{2}} E^{\frac{1}{2}}}{\pi^2 \hbar^3} \tag{1.2.1}$$

Where as for 2-D (quantum well) nanostructure where the two directions are for the movement of particles, while the third direction determines the quantum confinement

direction, the DOS is proportional to E^0 which is independent of energy and can be expressed by

$$D(E) = \frac{m}{\hbar^2 \pi} \tag{1.2.2}$$

Further squeezing of nanostructures in 2-D (quantum wire) which are free to move in only one direction and the two sides are confined. A large number of different structures have been grown and a wide range of interesting applications have been suggested, including electronic components, sensors, and light emitting components (lasers). And the DOS which is proportional to $E^{\frac{-1}{2}}$ is given by

$$D(E) = \frac{2^{\frac{1}{2}} m_e^{\frac{1}{2}} E^{\frac{-1}{2}}}{\pi \hbar} \tag{1.2.3}$$

Finally, for a zero dimensional system (quantum dot), the confinement is along all three dimensions and the DOS becomes a delta function [10]. Fig.1.4 shows DOS vs. energy for different dimensions.

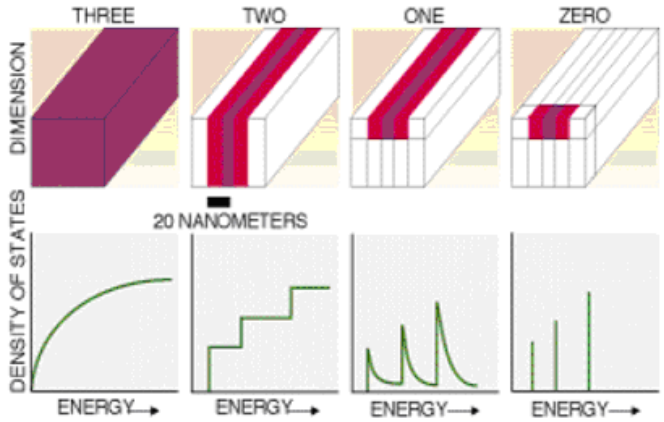

Figure 1.4: Densities of states for one band of semiconductor structure of 3, 2, 1 and 0 dimensions([10]).

Thus Fig.1.4 illustrates DOS in different dimensions varies as a function of energy as one goes from bulk to dot size (in the 3-D case the energy levels are continuous, while in the 0-D or molecular limit the levels are discrete) where their optical and electronic properties are dramatically modified due to the electron confinement in nanostructures that exhibit low-dimensional behaviors which mainly pronounces QCE.

1.3 Energy gap of nanostructures

The size quantization effect that has been looked into at great lengths only recently leads to an important change in various properties such as electrical property, optical transitions, conductivity, magnetization, etc. These different behaviors of most materials reflect the different character of the band gap i.e. the difference in energy between the lowest point of empty conduction band and the highest fulfilled point of the valence band [11].

Therefore downscaling of purely classical bulk material properties can lead to dramatic changes in behaviour in the nanoscale. Nevertheless the most exciting effects in the nanorealm where quantum physics comes into play and leads to completely new kinds of behaviour causes the band gap (E_g) to expand which means size quantization effect increases the energetic gap between the highest occupied and lowest unoccupied molecular orbitals (HOMO-LUMO gap), shifting the band gap from 1.12 eV in bulk Si all the way in to nano clusters as shown in Fig.1.5 [12].

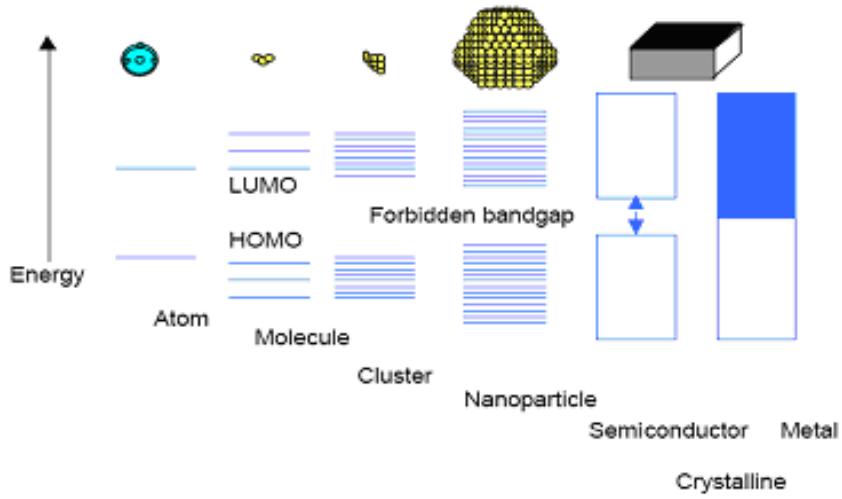

Figure 1.5: Size quantization effect. Electronic state transition from bulk to small cluster ([12]).

Different approaches exist in the theoretical modeling of the band structure of Si nanocrystals (linear combination of atomic orbitals, effective mass, tight binding), but all models lead to an increase of the band gap with decreasing crystallite size due to the carrier confinement (Fig.1.5). The change in band gap is observable as the nanocrystal size becomes smaller than 10 nm.

Effective mass model (EMM) is a method for approximating the band structure of solid using free electron like formalism. The free electron energy wave vector relation can be thought of as defining a mass m which determine the curvature of the band.

$$E = \frac{\hbar^2 k^2}{2m} \tag{1.3.1}$$

We assume a direct band gap semiconductor with the band gap at k = 0 and the definition for effective mass tensor is given by

$$M_{ij} = \frac{\hbar^2}{\frac{d^2 E}{dk_i dk_j}} \tag{1.3.2}$$

Near K = 0 at the bottom of the conduction band the tensor is nearly isotropic with an average diagonal element m_e, giving the energy of an electron in a given k state as

$$E_e(k) = E_c + \frac{\hbar^2 k^2}{2m*_e} \tag{1.3.3}$$

where E_c is the energy of the bottom of the conduction band. The effective mass for missing electron or hole in the valence band by the curvature of that band giving the energy of the hole in a given k state to be describe as

$$E_h(k) = E_v - \frac{\hbar^2 k^2}{2m*_h} \tag{1.3.4}$$

where E_v is the energy of the top of the valence band. The sign change is introduced to ensure that the hole effective mass is positive. So EMM can be illustrated by a simple case of confinement in a nanocrystal with linear dimensions L_x, L_y and L_z, where the band gap is given by the expression

$$E_{nc} = E_e(k) - E_h(k) = E_{bulkSi} + (\frac{\hbar^2\pi^2}{2})(\frac{1}{m*_e} + \frac{1}{m*_h})(\frac{n_x^2}{L_x^2} + \frac{n_y^2}{L_y^2} + \frac{n_z^2}{L_z^2}) \tag{1.3.5}$$

Hence this is equivalent to

$$E_{nc} = E_{bulk} + \frac{(\hbar n\pi)^2}{d^2 2\mu} \tag{1.3.6}$$

where E_{bulk}=1.12 ev , μ is reduced mass i.e $1/\mu = 1/m*_e + 1/m*_h$ while $m*_e$ and $m*_h$ are respectively the effective mass of electrons and holes. Based on this expression, the energy which is generated due to an electron and hole pair, increases as the size of the quantum wire decreases as shown in Fig.1.6 [13].

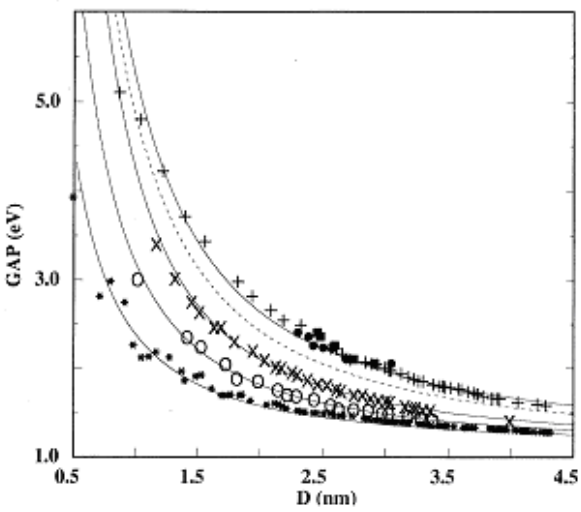

Figure 1.6: Calculated optical band gap energies for various Si crystallites (+) or wires (*,x,o) with respect to their diameter ([13]).

Thus band gap increases when the quantum wire decreased and the energy bands gradually convert into discrete molecular electronic levels. If the particle size is less than the De Broglie wavelength of the electrons, the charge carriers may be treated quantum mechanically. The quantization effect that enhances the optical gap is routinely observed for clusters ranging from 1 nm to almost 10 nm which significantly alter the material's structural, optical and electronic properties. Therefore among these different properties we are going to focus on optical properties that we will discuss in the next chapter.

1.4 Thesis organization

In this thesis we study the optical property of nanoporous silicon (np-si) quantum wires by determining the PL intensity as a function of energy upshift to formulate Gaussian line shape. In this study the PL is considered due to quantum confinement model.

The thesis is organized as follows. A broad introduction that deals with silicon nanostructures and with the quantum confinement effect is discussed. The optical properties of nanostructure semiconductors and how the PL is behaving in the direct band gap is thrash out in chapter 2. Chapter 3 will be devoted to the behavior of nanoporous Si (np-Si) and how the quantum confinement affects the photoluminescence of np-Si. We calculate the PL intensity as a function of energy upshift, different size distribution and wavelength to formulate the Gaussian model. In Chapter 4 we will discuss the results based up on our expressions with the framework of the quantum confinement model and give the summary and conclusion in Chapter 5.

Chapter 2

Optical behavior of semiconductor nanostructure and photoluminescence

In this chapter we are going to deal with the electron-hole exchange interaction that plays crucial role in the description of the basic optical properties of semiconductor nanostructure and also we will discuss how the photoluminescence behaves in the direct band gap semiconductor.

2.1 Optical properties of nanostructures

Most of the semiconductor properties, such as intrinsic conductivity, electronic transitions or optical transitions depend on the band gap. Any change of the gap significantly alters the materials physics. Thus, conduction in such materials requires a finite energy to promote the transition from the valance band to the conduction band either in the direct or indirect band gap way [14]. Let's see the difference between the two gaps.

In the direct absorption process, a photon is absorbed by the crystal with the creation of an electron-hole pair. Semiconductors using this phenomenon have their valence band maxima and their conduction band minima corresponding to the same momentum and are called direct band gap materials. Here the probability of radiative recombination is high which involves the emission of photons and has short radiative life time (in the order of μs). For such materials, $E_g = \hbar\omega_g$ where ω_g is the absorption frequency that determines the energy gap as shown below [15].

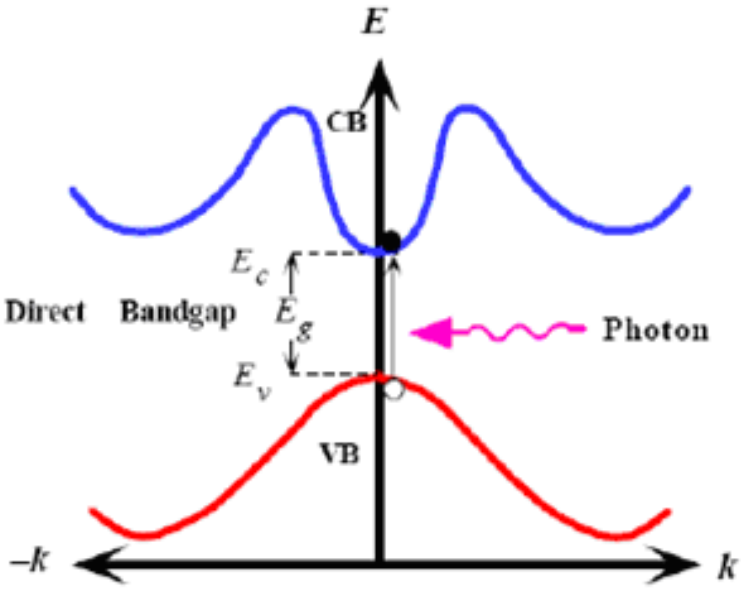

Figure 2.1: Direct photon absorption between valence band and conduction band ([15]).

As can be seen from Fig.2.1 it is drawn vertically with no significant change of k, because the absorbed photon has a very small wave vector.

In the indirect absorption process, the band gap involves electrons and holes separated by a wave vector k_c i.e. the maximum of valence band and minimum of conduction band do not correspond to the same momentum(not vertically aligned) are called

indirect band gap. Since the momentum of a photon is very small compared to the crystal momentum; the optical process should conserve the momentum of the electron. The energy of the excited carrier can be totaly dissipated by phonon interaction alone. The excited electron must lose an amount of energy corresponding to the gap and this would require the simultaneous creation of many phonons in order to dissipate the electrons energy. The conservation of momentum is phonon assisted. For instance with in the framework of band theory of solids; silicon has an indirect band gap which causes a very long radiative lifetime (ms) for excited electron-hole pairs. Therefore competing nonradiative recombination prevails and causes most of the excited electron-hole pairs to recombine nonradiatively. In addition, when the number of excited electron-holes increases other non-radiative recombination processes start to play a role[16].

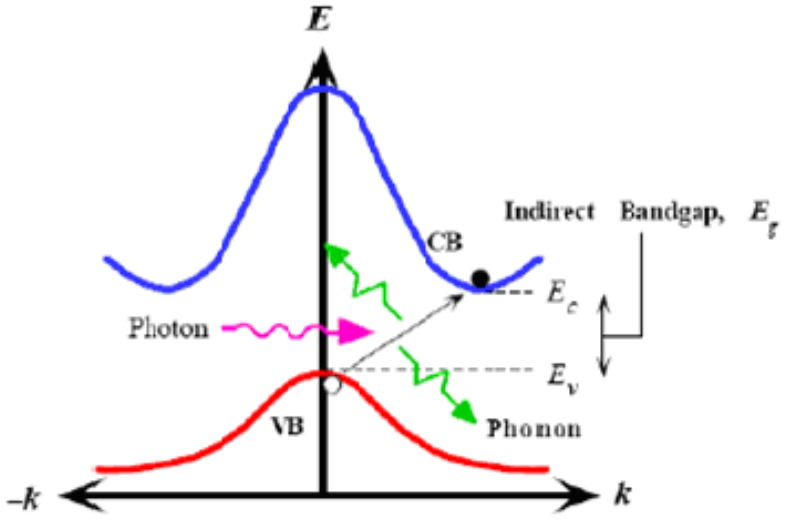

Figure 2.2: Indirect photon absorption between valence band and conduction band ([15]).

As can be seen from Fig.2.2 for this type of band gap a direct photon transition at the energy of minimum gap can satisfy the requirement of conservation wave vectors, because photon wave vectors are negligible at the energy range of interest. But if phonon of wave vector K and frequency Ω is created in the process, then we can have $\hbar\omega_g = E_g + \hbar\Omega$. The phonon energy $\hbar\Omega$ is, in general, much less than E_g.

Basically as electrons are excited from the lower valence band to the upper conduction band, holes are left behind the valence band. The de-excitation of electrons by making a transition from the bottom of the conduction to the top of the valence band is band gap recombination. The electron-hole bound pairs are bound together by electrostatic interaction created during the recombination process are known as excitons [17]. These are unstable against the ultimate recombination process in which the electrons drops in to the hole. When an electron-hole pair is created by absorption of photon, the absorption spectrum contains sharp lines just below the band gap energy and these lines are due to exciton levels. Hence exciton recombination is an important feature of photoluminescence [18].

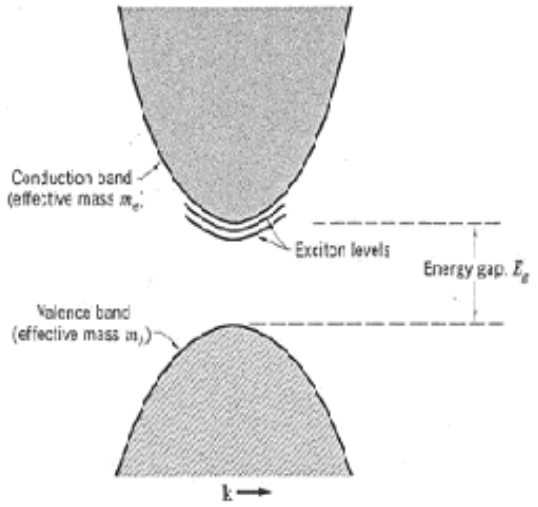

Figure 2.3: Schematic diagram of exciton levels in semiconductors ([15]).

Generally we can say silicon is an efficient light emitter semiconductor due to its indirect band gap which renders very improbable radiative transition with respect to non-radiative ones. To beat this inefficiency, one can reduce its size to few nanometers to obtain quantum confinement of the exited carriers that causes the material's optical gap to widen that changes the band gap in to direct. As a consequence, strong visible luminescence at room temperature is emitted from Si nanostructures.

2.2 Origin of Photoluminescence

To describe the origin of photoluminescence (PL) phenomena from nanoSi structures, consider nanoSi as an ensemble of nanomertic size spherical particles, having a well defined size distribution. The optical band gap widening in the crystallites is considered due to QCE in nanoparticles. We assume that both photo excitation and photo emission processes for electron -hole pairs occur inside the nanosilicon. And these

nanosilicon particles with diameters, d, less than $\sim$ 5nm exhibit strong photoluminescence (PL) at room temperature [19] which is a result of a significant overlap in electron and hole wave functions. However the electron-hole exchange interaction can be considered as a very weak perturbation in bulk semiconductors. It weakly modifies only the structure and energy of the exciton and does not play any role in the optical transitions. Recently it has been noticed that the electron-hole exchange interaction play a vital role in the description of the basic optical properties of nanocrystaline assemblies [20].

Therefore PL is a process in which a substance absorbs photons (electromagnetic radiation) and then re-radiates photons. Quantum mechanically, this can be described as an excitation to a higher energy state and then a return to a lower energy state accompanied by the emission of a photon [21].

Generally, silicon nanocrystallites grown by different methods exhibit strong photoluminescence in the red region and progressively shift towards the blue when the mean size decreases. Depending on the size, the photoluminescence of silicon nanocrystals can be tuned from the near infrared (1.38 eV) to the ultraviolet (3.02 eV) i.e due to QCE as shown in Fig.2.4.

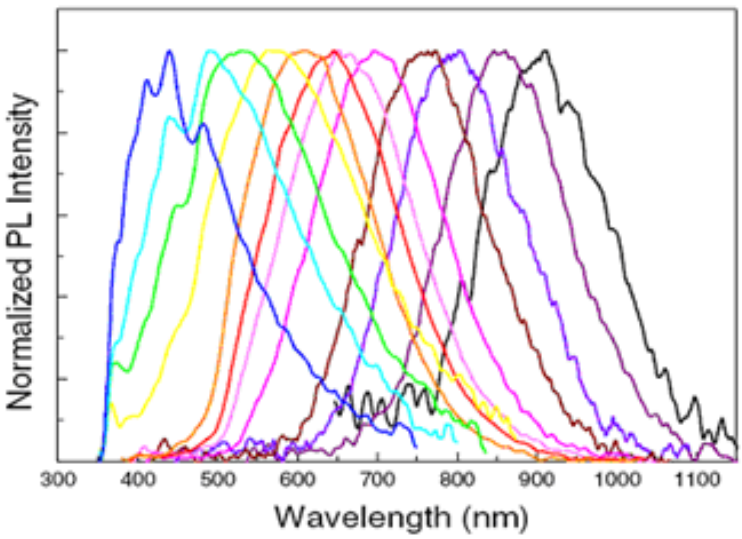

Figure 2.4: Room-temperature photoluminescence spectra of silicon nanocrystallites ([13]).

As can be seen from Fig.2.4, changing the photoluminescence emission from $\sim$ 410 to 900nm is possible by altering the size of the silicon nanocrystals.

The excitation energy and intensity are chosen to probe different regions and excitation concentrations in the nanostructure. Moreover PL investigations can be used to characterize a variety of material parameters as a result of electron-hole pair recombination in different mechanisms where we are going see it in the next subsection.

2.3 Photoluminescence mechanisms

Some literatures mentioned that more than one type of mechanism models are needed in interpreting PL from porous silicon (p-Si). In the years between 1992 and 1997 there have been at least 24 models different from quantum confinement model suggested [22]. But here we are not going to address all models; however, we describe in this dissertation the first and most commonly mentioned PL mechanism model, Quantum Confinement Model (QCM). Canham's first report states that strong visible PL from porous silicon at room temperature exists, with an inverse correlation of the optical gap with the nanoparticle size. While this finding provides an important piece of evidence for QCM .

2.3.1 Quantum confinement model

The first mechanism model suggested explaining the visible light emission in porous Si is the quantum confinement model (QCM) or (luminescent centerd model). In this model, the light emission process itself was assumed to be the result of carrier recombination within quantum confined porous Si (P-Si), (i.e. both the optical excitation and recombination takes place inside the nanosilicon particle) and the particle's mean size is inversely scale with the energy of the PL which is similar to the electron-hole recombination but in this case the emission energy E_g would be replaced by E_{QC}, the energy due to quantum confinement effect, which could be significantly above 1.12 eV. Due to the quantum confinement of the carriers the PL mechanism strongly includes the QC effect.

Though several experimental and theorethical evidences supporting QCM are discussed in many literatures concerning this model, it is clear that other interpretations are just as valid. One of the most significant problems with the QCM is that no convincing experimental data exist showing the direct relationship between the PL energy and the particle size in p-Si. The relation ship between particle size and PL peak energy in p-Si, is confirmed by using optical absorption, Raman spectroscopy and photoluminescence [23].

Thus PL is one forms of luminescence (light emission) and is distinguished by photoexcitation (excitation by photons) where its characteristics changed as the wavelength of emission changes from ultraviolet wavelengths to infrared wavelength along with the QCE that we are going to deal with it's formulation using Gaussian model in the next chapter.

Chapter 3

Formulation of Gaussian model for photoluminescence

In this chapter we are going to discuss the behavior of nanoporous Si (nP-Si), and we will discuss how the quantum confinement affects the photoluminescence (PL) of nP-Si. Finally we will calculate the PL intensity as a function of energy upshift to formulate the Gaussian model.

3.1 Behavior of nanoporous Si

Ever since the discovery of photoluminescence in an indirect bandgap material like Si upon electrochemically etching a Si wafer as reported by Leigh Canham in 1990, there has been a tremendous interest in the study of these electrochemically etched crystalline Si materials, called porous Silicon (P-Si). It is sponge like structure with features (i.e.pores and undulating wires) with size of the order of few nm and has interesting characteristics such as larger surface area to volume ratio, highly nanoporous structure (controllable property), versatile, unstable due to porosity, which suggest other potential applications besides optical applications like filters, catalyst supports, chemical sensors, biological applications, antireflection coatings in solar cells etc [24].

Among the many different Si-based materials studied for their luminescence properties, porous silicon (P-Si) has proved to be one of the most promising; as it emits light at room temperature in the visible range with high quantum efficiency. Then the properties of nP-Si structures are of increasing importance for a fundamental understanding of nano systems as well as from a practical point of view to understand and control the materials fabrication processes [25]. Recently, a correlation has been demonstrated between the photoluminescence (PL) energy of nP-Si and the size of its remnant nanoscale silicon units.

The strong photoluminescence from nP-Si has evoked a great deal of interest due to its potential applications in optoelectronic device [26]. Thus, an indepth study of nP-Si structures may throw light on fundamental properties related to the origin of room temperature photoluminescence with quantum confinement effect and the size of the pores.

3.2 Effect of quantum confinement on photoluminescence of nanoporous Si

As we discuss earlier photoluminescence (PL) is a powerful, non-destructive technique for measuring the optical properties of a sample. A laser beam is directed onto the sample and, if of sufficient energy, photons are absorbed and electronic excitations is created. Eventually, these excitations relax and the electrons return to the ground state. The relaxation can occur radiatively with the emission of a photon or nonradiatively [27]. Therefore PL measures the radiative recombination and as such is a sensitive probe of electronic states.

NP-Si exhibits efficient room temperature luminescence in the visible range. The complexity in the structure of this material has led to the formation of many different models to explain its luminescence but we are going to see the first and most favorable explanation for the visible emission in nP-Si i.e. the quantum confinement of excitons in nanometer-sized silicon. The origin of photoluminescence from nP-Si remains controversial. Some researchers have stated that P-Si has a wire like structure and that the PL is due to the two- dimensional carrier confinement in it. Others thought that it is due to the luminescence from amorphous Si, or molecules attached to Si. Recently, we have revealed that nP-si has a disordered structure, and the PL from nP-Si is most likely due to the quantum confinement in the nano-sized Si clusters. It is necessary to pinpoint the real microstructure of P-Si that emits visible light for understanding the mechanism of luminescent nP-Si [28].

Hence Light emission from nanoporous silicon due to QCE occurs mainly in the visible region of the electromagnetic spectrum. The emission has the unique property that the wavelength of the emitted light can be changed simply by increasing or decreasing the porosity of the material. For example, a highly porous sample (70-80 percent porosity) will emit blue light while a less porous sample (40 percent) will emit red light. Therefore the PL peak energy increases with decreasing diameter, in accordance with the quantum confinement effect.

Generally, it is believed that the efficient luminescence in P-Si can be assigned to its nanostructures, whose band gap is blue-shifted because of the quantum confinement (QC) effect. For this reason, it is necessary to understand in detail the electronic states and optical properties of Si nanostructures in order to clarify the mechanism of the efficient luminescence.

3.3 Derivation of PL spectra as a function of energy upshift

The observation of visible PL in a variety of semiconductor nanocrystallites has fueled a large body of research work in the past decade. The photoluminescence from such systems are broad, and often asymmetric about the peak energy. Our aim is to explain this PL spectrum. There exist two classes of explanation for the origin of visible PL in nP-Si: (i) the quantum confinement model in which luminescence is due to electronic confinement in the columnar like structure of porous Si and (ii) the chemical model in which the large surface area presented by nP-Si support luminescing siloxenes. But we work here with in the quantum confinement model but avoid the oversimplifying assumptions made by some of its proponents [29].

To compute a general expression for the PL spectrum, one needs to consider the crystallites sizes in the system. In this work, we provide a simple theoretical framework to calculate the spectral line shape.

The PL intensity from nanoporous silicon quantum wire having size distribution $N_{e(d)}$ will be obtained by summing the contributions from all the columns having diameter d. The PL intensity from crystallites of diameter d is given by

$$\mathrm{I(d)} \ \alpha \ P(d)N_e(d)$$

Columns of mean diameter d_o in the nanometer range have been reported by several independent groups. The growth of these columns is a stochastic process and it appears reasonable to assume columns of Si with a Gaussian distribution of diameter

d centered around a mean diameter:

$$p_d = \frac{1}{\sqrt{2\pi}\sigma} e^{\frac{-(d-d_o)^2}{2\sigma^2}} \tag{3.3.1}$$

where d_o is the mean diameter and σ is the variance of the column. The number of electrons in a column of diameter d participating in the radiative process is proportional to d^2 and the heights of the columns depends only on the growth time and are approximately the same. Hence

$$N_e = N_e(d) = bd^2, \tag{3.3.2}$$

where b is constant.

The probability distribution of electrons participating for nP-Si sample consisting of varying column diameter in the PL process is given by a product of the above two expressions i.e.

$$I(d) = \frac{1}{\sqrt{2\pi}\sigma} bd^2 e^{\frac{-(d-d_o)^2}{2\sigma^2}}, \tag{3.3.3}$$

With in a simple effective-mass theory (in the quantum confinement model) the PL process is attributed to the energy upshift of electrons and is proportional to $\frac{1}{d^2}$.

$$\hbar\omega = E_g - E_b + \frac{c}{d^2}, \tag{3.3.4}$$

Where E_g is the bulk Si gap (1.12 eV), E_b is the exciton binding energy, and c is an appropriately dimensioned constant [30].

The energy upshift due to confinement ΔE is

$$\Delta E = \hbar\omega - (E_g - E_b), \tag{3.3.5}$$

This is equivalent to:

$$\Delta E = \frac{hc}{\lambda} - (E_g - E_b) \text{ and } \Delta E_o = \frac{c}{d_o^2}$$

where we have also paused to define mean upshift energy E_o related to the mean column diameter d_o.

The PL line shape is then determined by transforming eqn (3.3.3) to the energy axis using fourier transformation which is given by

$$I(\Delta E) = \frac{1}{\sqrt{2\pi}\sigma} b \int \delta(\Delta E - \frac{c}{d^2}) d^2 e^{\frac{-(d-d_o)^2}{2\sigma^2}} d(d) \tag{3.3.6}$$

Letting $E - \frac{c}{d^2} = f(x)$, $d^2 e^{\frac{-(d-d_o)^2}{2\sigma^2}} = g(x)$ and $d = x$ then we can write the intensity as

$$I(\Delta E) = \frac{1}{\sqrt{2\pi}\sigma} b \int \delta(f(x)) g(x) dx \tag{3.3.7}$$

Therefore using Dirac delta property eqn.(3.3.7) can be integrated as

$$I(\Delta E) = \frac{1}{\sqrt{2\pi}\sigma} b \int \delta(f(x)) g(x) dx = \frac{1}{\sqrt{2\pi}\sigma} b \sum \frac{g(x)}{\dot{f}(x)} \tag{3.3.8}$$

And from $f(x) = 0$, $x = \sqrt{\frac{c}{\Delta E}}$ and $\dot{f}(x) = 2cx^{-3}$ gives

$$I(\Delta E) = \frac{b}{\sqrt{2\pi}\sigma} (\frac{1}{2\Delta E}) (\frac{c}{\Delta E})^{\frac{3}{2}} exp \frac{-1}{2} (\frac{d_o}{\sigma})^2 [\sqrt{\frac{c}{\Delta E d_o^2}} - 1]^2 \tag{3.3.9}$$

Then recalling $\Delta E_o = \frac{c}{d_o^2}$, yields for the intensity which is expressed by

$$I(\Delta E) = \frac{b}{\sqrt{2\pi}\sigma} (\frac{1}{2\Delta E}) (\frac{c}{\Delta E})^{\frac{3}{2}} exp \frac{-1}{2} (\frac{d_o}{\sigma})^2 [\sqrt{\frac{\Delta E_o}{\Delta E}} - 1]^2 \tag{3.3.10}$$

Thus the PL line shape is approximately Gaussian if σ is small. For finite σ the $\sqrt{\frac{1}{\Delta E}}$ factor in the exponential outweighs resulting in an asymmetric curve with the shoulder.

We need to note also that the mean energy of the upshift E_o and the location of the PL peak are not the same. To see this let the PL peak position $[E_p = \hbar\omega_p - (E_g - E_b)]$ is given by the maxima determining by setting

$$\dot{I}(\Delta E) = \frac{b}{\sqrt{2\pi}\sigma}(\frac{1}{2\Delta E})(\frac{c}{\Delta E})^{\frac{3}{2}} exp\frac{-1}{2}(\frac{d_o}{\sigma})^2[\sqrt{\frac{\Delta E_o}{\Delta E}} - 1]^2 = 0 \tag{3.3.11}$$

This yields

$$\Delta E_p = \Delta E_o[\frac{1}{10}(\frac{d_o}{\sigma})^2(-1 + \sqrt{1 + 20(\frac{\sigma}{d_o})^2})^2] \tag{3.3.12}$$

This equation implicitly contains the dependence of the peak energy E_p on the mean crystallite size d_o. To find the relationship of E_p and E_o we can write for typical values of [31] $d_o = 30$

A^o, $\sigma = 3$ $\mathcal{A}^o$, and for $\frac{\sigma}{d_o} \longrightarrow 0$; eqn. (3.3.12) becomes

$$\Delta E_p = \Delta E_o[1 - 5(\tfrac{\sigma}{d_o})^2]^2 \Rightarrow \Delta E_p = \Delta E_o$$

This can be written as

$$\Delta E_p = \Delta E_o[1 - 10(\tfrac{\sigma}{d_o})^2]$$

For the above values ($d_o = 30$ A^o, $\sigma = 3$ A^o), $\frac{\sigma}{d_o} \simeq 0.1$, and $E_p \simeq 0.9E_o$. Thus there is down shift.

The peak in PL intensity can be written as

$$I(\Delta E_p) = \tfrac{b}{\sqrt{2\pi}\sigma}(\tfrac{1}{2\Delta E_p})(\tfrac{c}{\Delta E_p})^{\frac{3}{2}} exp\tfrac{-1}{2}(\tfrac{d_o}{\sigma})^2[\sqrt{\tfrac{\Delta E_o}{\Delta E_p}} - 1]^2$$

We can obtain an approximate expression for the full width at half maximum (FWHM) (ΔE_{FWHM}) of the PL spectrum if the prefactor energy dependence $E^{\frac{-5}{2}}$ is ignored [30, 31]. Moreover from difference between two points point of view, we can write for the energy of FWHM as

$$\Delta E_{FWHM} = \Delta E_o[(1 - (\tfrac{\sigma}{d_o}))^{-2} - (1 + (\tfrac{\sigma}{d_o}))^{-2}]$$

Using quantum confinement model ($E = \frac{c}{d^2}$), for small $(\frac{\sigma}{d_o})$ we can simplify it as

$$\Delta E_{FWHM} = \frac{4\Delta E_o \sigma}{d_o} \tag{3.3.13}$$

Thus our work is based on quantum confinement model where the PL peak is sought to explain and we believe that the disorder plays a key role and model it by a distribution of crystallite sizes.

Chapter 4

Results and discussions

In the previous chapter we have seen how the PL spectrum varies with the diameter of the quantum wires and the energy upshift. In this chapter we investigate the results based on our expression in the previous chapter. The plots are generated from the relation we obtain in eqn(3.3.10) using Fortran code. In addition, we use the energy gap vs.diameter as an input parameter from pseudopotential simulation (PPA) and the tight binding model (TB) fit to our model and generate PL. The numerical values of important variables in our calculation are as follows: The band gap of bulk Si ($E_g \simeq 1.12\ eV$), the exciton binding energy ($E_b \simeq 0.14\ eV$) and the constant c associated with the confinement energy is 485.816 eV A^{o2} ([30]).

4.1 Photoluminescence (PL) spectra against energy upshift

The PL spectra were simulated using $I(\Delta E) = \frac{b}{\sqrt{2\pi}\sigma}(\frac{1}{2\Delta E})(\frac{c}{\Delta E})^{\frac{3}{2}} exp\frac{-1}{2}(\frac{d_o}{\sigma})^2[\sqrt{\frac{\Delta E_o}{\Delta E}} - 1]^2$ with the typical values of d_o and σ found in the nP-Si samples. Then the calculated PL spectra for fixed sample mean diameter of $d_o = 4$ nm and $\sigma = 0.2$ nm are shown in Fig.4.1.

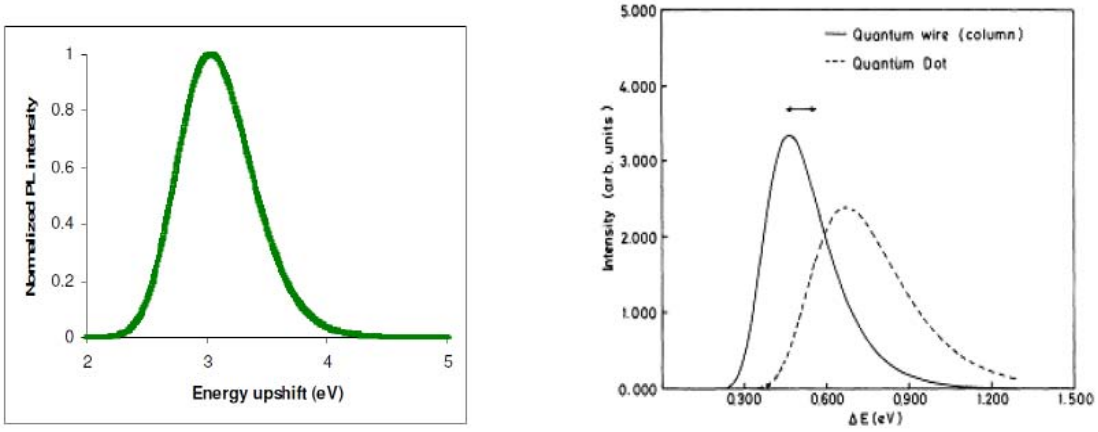

Figure 4.1: Theoretical PL spectra vs. energy upshift with fixed mean diameter d_o= 4 nm and variance $\sigma = 0.2$ nm (right) and experimental (left),([30]).

Fig.4.1 depicts that the PL intensity which has fixed and small variance of 0.2 nm has gaussian line shape that has PL peak position at $\simeq$ 2.73 eV and has FWHM $\simeq$ 0.608 eV.

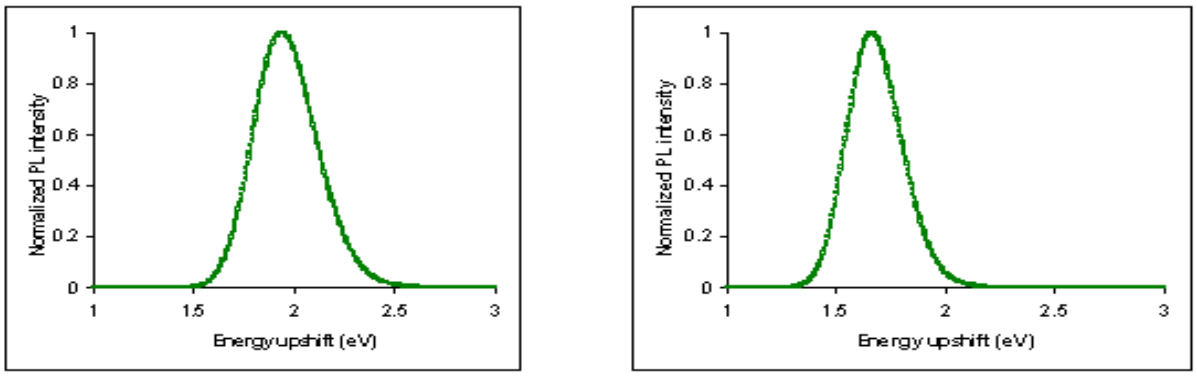

Figure 4.2: PL spectra (left) and (right) using energy gap vs. size as input parameter from PPA and TB with fixed mean diameter $d_o = 5.0$ nm and d_o= 5.4 nm respectively of fixed variance of $\sigma = 0.2$ nm for both.

In Fig.4.2 the PL spectra is plotted with the help of eqn.(3.3.10) taking data from energy gap vs. size as an input parameter from PPA of fixed mean diameter $d_o = 5$ nm and fixed variance. And similarly from TB also we take fixed mean diameter of $d_o = 5.4$ nm and fixed variance. Thus, the PL spectrum is Gaussian that is in a good agreement to our theoretical PL spectrum model which has FWHM $\simeq 0.31$ eV and $\simeq 0.28$ eV respectively. It is important to note that to obtain Gaussian line shape of PL spectrum, variance should be small. The same PL spectrum is also observed experimentally.

4.2 Photoluminescence (PL) spectra against wavelength

Here also the PL spectrum was obtained from eqn. (3.3.10) with fixed value of variance. The calculated PL spectra for fixed $\sigma = 0.16$ nm with different mean diameters of the wires and energy upshift are shown in Fig.4.3. Note that $\hbar\omega = \frac{1240}{\lambda}$ and recall that $\hbar\omega = \Delta E - (E_g - E_b)$ from eqn.(3.3.4).

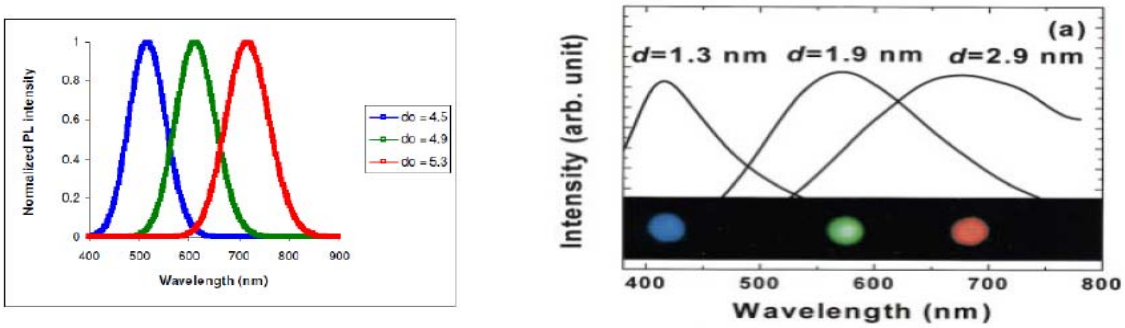

Figure 4.3: Theoretical PL spectra against wave length computed to wires with different mean diameters and fixed standard deviation of $\sigma = 0.16$ nm (right) and expermental,(left)([28]).

Interestingly, the PL line shape is altered significantly by the mean diameter of the wires. As shown from the Fig.4.3, as the diameter of the wire increases to 5.3 nm, the PL peak energy decrease as 2.16 eV, 1.82 eV and 1.56 eV respectively and the FWHM also decreases as 0.34 eV, 0.26 eV and 0.21 eV respectively but the wavelength increases as 517 nm, 614 nm and 717 nm though the energy upshift decreases. Thus the smallest one of the three different diameters (4.5 nm) has large energy upshift that emits blue light accompanied with an increase in PL intensity and the reverse is true for largest size (5.3 nm) i.e. it has small energy upshift that emits red light accompanied with the small PL peak energy. This indicates that the mean diameters of the columns being the dominant parameter governing the QCE, which plays a crucial role on PL peak energy and a wide range of luminescent wavelengths has been observed from near infrared to ultraviolet.

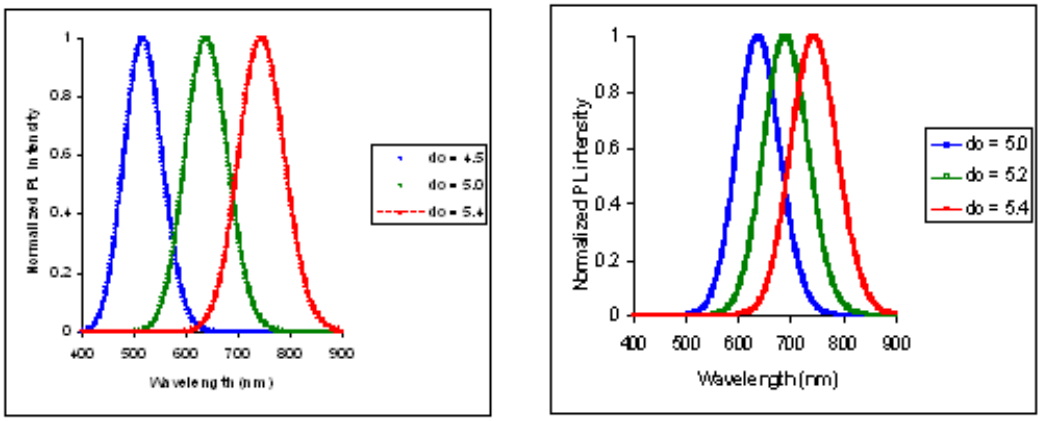

Figure 4.4: PL spectra (left) and (right) using energy gap vs. size as input parameter from PPA and TB respectively having normal size distribution with different mean size and fixed standard deviation $\sigma = 0.16$ nm which are fitted to our model.

We breed the graph in Fig.4.4 by taking three different mean diameters from energy gap vs. size as an input parameter from PPA and TB respectively to endorse our model with fixed standard deviation. Therefore as can be seen the graphs fit and exemplify the same characteristics to our model. Recent experiments are also in conformity with this observation. The PL spectra is very much sensitive to shape, size and nature of the nanostructure.

4.3 Photoluminescence (PL) spectra against energy upshift for different mean diameter

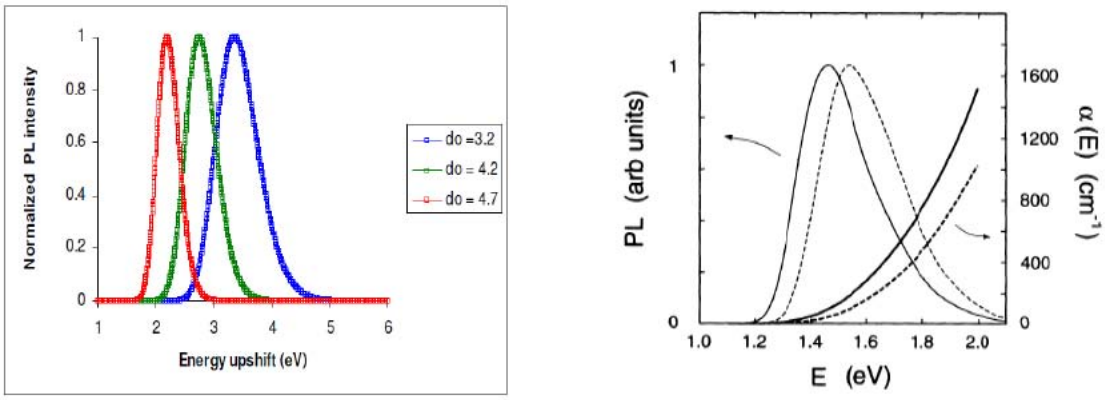

Figure 4.5: Normalized PL spectra computed for different mean diameter of column having fixed standard deviation σ of 0.2 nm. Spectra shown are for three different values of d_0.(right) and experiment (left) of 4.1 nm (solid line) and 3.4 nm (dashed line),([32]).

It is noted that the novel implications of quantum size effects on the energetic addresses new physical phenomena, which are qualitatively different from those of the bulk, i.e.in Fig. 4.5 as we increases the diameter to 4.7 nm, the Pl peak position decreases as 4.27 eV, 2.48 eV and 1.98 eV and the FWHM also decreases as 0.78 eV,

0.5 eV and 0.37 eV. Hence for the smallest size (3.2 nm), the energy upshift broadens and consequently its PL peak increases and emits blue light. Nevertheless for the largest size (4.7 nm) the energy upshift is small and emits red light. Thus, QCE is predominant for the strong and visible PL intensity.

We shall now present the energy gap against diameter of the column as an input parameter obtained from PPA and TB that strength QCE and our model. This data has been utilized to fit our PL spectra using Gaussian model.

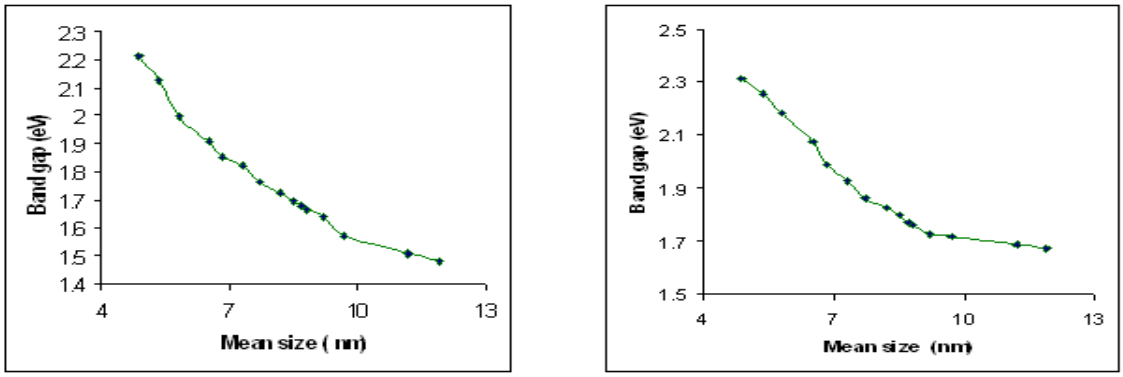

Figure 4.6: Band gap vs. mean diameter of column data from PPA and TB ([33]).

As can be seen from the above in both graphs we can figure out that the energy upshift decreases as the mean diameter of the quantum wires increases. Moreover in order to be more relevant we take three points from both graphs to our calculation eqn.(3.3.10) then obtain the following graphs.

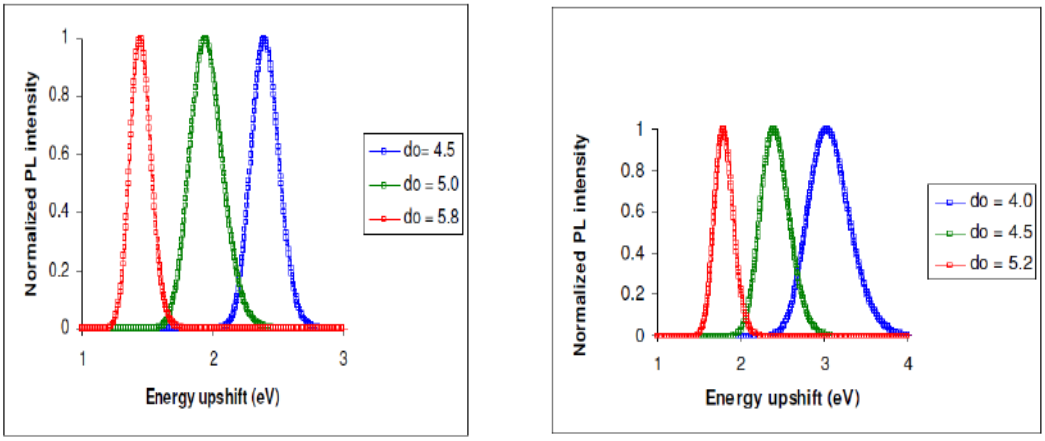

Figure 4.7: Normalized PL spectra using energy gap vs. size as an input parameter from PPA and TB respectively having different size distribution and fixed standard deviation of σ=0.16 nm. Spectra shown are for three different values of d_o.

Evidently Fig.4.7 illustrates the same characteristics that execute our model which generates from energy gap vs. diameter as an input parameter from PPA and TB. This implies that that they fit to our model interestingly. These results are also in agreement with other experimental and theoretical observation.

Recently people are doing an extended study of the size effects on the PL properties of different films, with the aim of addressing the issue of quantum confinement as an explanation for the PL characteristics of silicon nanostructures. it has been studied several samples with varying mean size and size distribution. The samples were characterized by different techniques studied is determined by time-of-flight mass spectrometry (TOFMS) without further size selection.The characteristics of the two sets of samples studied are summarized in Table 1.

Sample identifier	Average Size (nm)	PL maximum (nm)	PL maximum (eV)
A	3.44	680	1.82
B	3.46	610	2.03
C	3.88	710	1.75
D	4.05	750	1.65
E	4.45	800	1.55
-	-	-	-
K	2.8	635	1.95
L	3.2	725	1.71
M	3.6	~ 860	~ 1.44
N	4.8	≥ 900	≤ 1.35

Table 4.1: Characteristic parameters and PL properties of the different samples studied ([31]).

The first one (samples A-E) was deposited on a KBr substrate while the second one (samples K-N), which was synthesized and characterized later, was deposited on fused quartz substrates.As we see from table 1 it is noted that the PL is strongly dependent on size distribution. A change of the average size from 4.8 nm $\sim$ sample N, to 2.8 nm $\sim$ sample L, results maximum value of PL and for average size from 4.45 nm $\sim$ sample E to 3.44 nm $\sim$ sample B also results an increase in PL intensity except for sample A because of the frequency that is different from others.

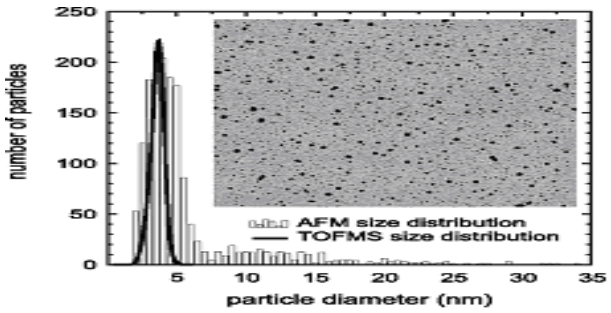

Figure 4.8: Size distribution derived from a 6x6 μm^2 AFM image compared with the size distribution measured by TOFMS during sample preparation([31]).

Homogenously distributed nanostructures with out any agglomeration are apparent on the AFM images and its result is in Fig.4.8 together with the size distribution measured by TOFMS during this preparation of the samples [31].

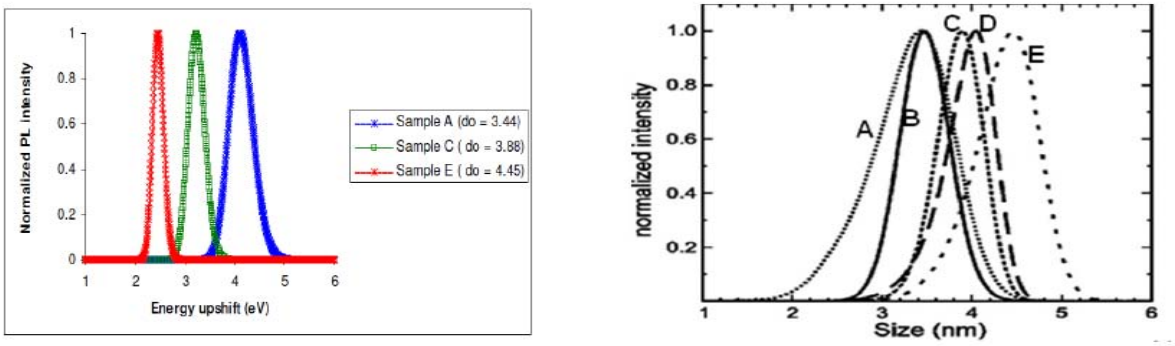

Figure 4.9: Normalized PL intensity vs. energy upshift for different mean size for the first sample with fixed variance of 0.1 nm ([31]).

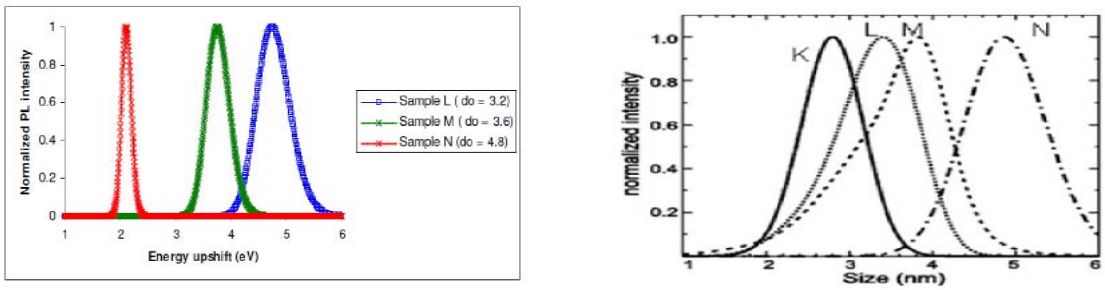

Figure 4.10: Normalized PL intensity vs. energy upshift for different mean size for the second sample with fixed variance of 0.1 nm ([31]).

Figures 4.9 a, b and 4.10 a, b depict that the PL spectra of the different samples studied together with their size distributions as measured by TOFMS. Hence 4.8 (a) and 4.9 (a) are generated from the experimental data of the first and the second sample to our calculation for comparison. Thus our model calculation has good

agreement with the experimental data except in the peak region. This might be due to different reasons such as the nature of the structure, the surrounding media effect, temperature etc.

Generally the quantum confinement effect increases the band gap of material as the size of quantum structure decreases, which results in a blue shift in optical luminescence and absorption energy. To demonstrate this effect, we measured photoluminescence of different Quantum wires sample with various mean diameters as we discuss earlier.

It is worth to mention that the application of our model requires physical understanding of the parameters used for the system under study. A quantitative agreement of the PL model with the experimental PL data depends on the exactness of the average crystallite size and its dispersion, exciton binding energy E_b, and also on the models that estimate band gap. We believe that our model could provide a nice qualitative picture of the observed PL. However, for detail nature of the PL spectra much more serious calculations are needed that cover complete and various descriptions of Si nanostructures. However with our model of Gaussian distribution of mean diameter of quantum wire we found an excellent qualitative match.

Chapter 5

Conclusions and future outlook

In this thesis work we have investigated the optical properties of nanoSi. NanoSi research is highly fertile with different technological possibilities that can fabricate using top-down and bottom-up approaches. Bulk silicon has a problem for light-emitting applications due to its indirect bandgap, while nanostructurizing of Si comprises porous silicon, quantum dots, quantum wells and nanoclusters that can exhibit strong photoluminescence at room temperature which is observed only after a drastic reduction of silicon size and has been related to quantum confinement effect that alters indirect bandgap to direct bandgap.We use a Fortran code to generate the graphs and it is attached in the appendix.

Quantum confinement (QC) is change of electronic and optical properties when the material sampled is of sufficiently small size - typically 10 nanometers or less. It widens the band gap that occurs when the nanostructures size become comparable to the Bohr exciton radius in bulk silicon. In order to characterize the physical properties like optical transitions in silicon nanostructures, the information about the density of states which depends on the dimensionality of the system is very crucial.

Silicon nanostructures have tremendous applications in the photoluminescence, optoelectronic and photonic devices. They can be easily integrated into silicon wafer processing and utilized for biological, chemical, optical sensors and memory devices. These can be grown by different methods that exhibit strong photoluminescence in the red region and progressively shift towards the blue when the mean size decreases. Depending on the size, the photoluminescence of nanocrystallites can be tuned from the near infrared to the ultraviolet.

We describe the origin of photoluminescence (PL) phenomena from nanoporous Si structures. And we assume that both photo excitation and photo emission processes for electron-hole pairs occur in the nanosilicon particles with diameters d, less than 6nm exhibit room temperature photoluminescence (PL) [18] which is a result of a significant overlap in electron and hole wave functions. Hence it is noticed that the electron-hole exchange interaction plays a vital role in the description of the basic optical properties of nanocrystaline assemblies.

nanoP-Si has been extensively studied experimentally as well as theoretically. The combination of experimental and theoretical results enables us to develop a consistent picture of P-Si luminescence. The strong PL of nP-Si is due to quantum confinement model that can be traced continuously and smoothly from the bulk silicon PL (infrared spectrum) to the visible spectrum.

We have used the energy gap vs. size as an input parameter from tight binding model and pseudopotential simulation to generate the PL spectra. It is however, worth to take the data from different samples studied together with their size distributions as measured by TOFMS. And then fit to our model to compare the experimental PL.

Our results are in conformity with some of the recent experimental and theoretical observations.

To compute the parameters of spectral line shape from nano porous silicon, one needs to consider the distribution of the mean diameters in the quantum wire.Though the shift in the PL peak with varying mean diameter is refused by other groups based on the experimental work, recently an attempt was made to explain this conflict on the basis of size distribution of nanocrystallites based on computer simulation study. Our model attempts to resolve the issues raised by these studies.

Thus, our result shows that the decrease in the mean diameter of nanoporous silicon quantum wire increases the band gap due to QCE giving strong PL. This is in good agreement with experimental results for nP-Si. In conclusion, our work presents a new approach for the PL line shape of nP-Si Gaussian. And our theoretical result confirms that low dimensional crystallites manifest strong PL. For the future, using this approach it is possible to study other related issues, such as temperature dependent on PL and EL can be incorporated in our model for both crystallites and porous si is also worth to look at.There is great demand of model conclusion to quantify most of the optical parameters (like oscillator strength, radiative life time) for applied interest.And Effect of Exciton and porosity is important to look at. We believe that Gaussian model looking at PL of nP-Si quantum wires is new observation by us that provide very good qualitative agreement with other observations. So it is open for further studies.

Appendix : Computational matters

Overview of the working of the programs

We use eqn(3.3.10) i.e. $I(\Delta E) = \frac{b}{\sqrt{2\pi}\sigma}(\frac{1}{2\Delta E})(\frac{c}{\Delta E})^{\frac{3}{2}} exp\frac{-1}{2}(\frac{d_o}{\sigma})^2[\sqrt{\frac{\Delta E_o}{\Delta E}} - 1]^2$, that provides the PL intensity as a function of energy upshift and we generate the graphs based on our calculations using FORTRAN-77 programs.All programs share the following constant variables.

$c = 485.816 \;\; eVA^{o2}$ is the dimensionality constant.

$E_g = 1.12 \;\; eV$ is energy gap of bulk silicon.

$E_b = 0.14 \;\; eV$ is exciton binding energy.

And ΔE_o = b $= \frac{c}{d_o^2}$ is mean energy upshift, ΔE is energy upshift, σ is standard deviation, d_o is sample mean diameter and we let for $sigma = a$, $\Delta E_o = b$, $d_o = d$, $\Delta E = e$, and λ= G. Hence based on the above equation the following various graphs are generated in the results and discussions part accordingly.

A.1 Gauss.F

This programme was used to produce the graph of PL intensity vs.energy upshift for fixed mean diameter and standard deviation.

```
real a, b, c, d, e, z, f, s
open(1,file='PL1.dat',status='unknown')
do e =1,6,.005
```

pi= 4.0 $\star$ tan(1.0)

a = 0.2

c=48.58

d= 4.0

b = c/(d**2)

$v = (\frac{d}{a}) * *2$

$s = (sqrt(\frac{b}{e} - 1)$

f=s**2

z=exp(-0.5*(v)*f)

$write(1, *)e, z$

$print * e, z$

enddo

end

Where e=ΔE is energy upshift (x-axis) and z is PL intensity (y-axis) of Fig.4.1. Similarly form the energy gap vs. size data from PPA and TB we simply change the mean diameter taking 5 nm and 5.4 nm and run the programme to generate Fig.4.2 respectively.

A.2 PLwave.F

This programme is the graph for PL intensity vs. wavelength for different mean diameters and fixed standard deviation.

real a, b, c, d, e, z, f, s

open(1,file='PL2.dat',status='unknown')

do G =400,900,.06

pi= 4.0 $\star$ tan(1.0)

a = 0.16

c=48.58

d =4.5

b = c/(d**2)

e = $\frac{1240}{G}$

$v = (\frac{d}{a}) * *2$

$s = (sqrt(\frac{b}{e} - 1)$

f=s**2

z=exp(-0.5*(v)*f)

$write(1, *)G, z$

$print*, G, z$

enddo

end

Where G=λ is wavelength (x-axis) and z is PL intensity (y-axis). Similarly run this programme for mean diameter of 4.9 nm and 5.3 nm to generate Fig.4.3.And also we take three different mean diameters from energy gap vs. size data from PPA and TB i.e 4.5 nm,5.0 nm,5.4 nm and 5.0 nm, 5.2 nm, 5.4 nm respectively and run this programme to obtain Fig.4.4.

A.3 PLdifmean.F

This programme produce the graph for PL intensity vs. energy upshift for different mean diameters having fixed standard deviation.

real a, b, c, d, e, z, f, s

open(1,file='PL3.dat',status='unknown')

do e = 1,6,.005

pi= 4.0 $\star$ tan(1.0)

a = 0.2

c=48.58

d =3.2

b = c/(d**2)

$v = (\frac{d}{a}) * *2$

$s = (sqrt(\frac{b}{a} - 1)$

f=s**2

z=exp(-0.5*(v)*f)

$write(1, *)e, z$

$print*, e, z$

enddo

end

Where e=ΔE is energy upshift (x-axis) and z=PL intensity (y-axis). Similarly run this programme for mean diameter of 4.2 nm and 4.7 nm to generate Fig.4.5. Moreover we take three different mean diameters having fixed standard deviation from energy gap vs. size data from PPA and TB of values 4.5 nm, 5.0 nm, 5.8 nm and 4.4 nm, 4.5 nm, 5.2 nm respectively to generate Fig.4.7. And also to validate our model we take from two experimental samples of mean diameters 3.44 nm, 3.88 nm, 4.45 nm and 3.2 nm, 3.6 nm, 4.8 nm from the first and second samples (from table 1) having fixed standard deviation of 0.1 nm to generate Fig.4.9 and 4.10 respectively.

Glossary

PL - Photoluminescence

P-Si - Porous silicon

nP-Si - Nanoporous Si

QC - Quantum confinement

QCE - Quantum confinement effect

EBR - Exciton bohr radius

DOS - Density of states

HOMO - Higher occupied molecular orbital

LUMO - Lower unoccupied molecular orbital

QCM - Quantum confinement model

EMM - Effective mass model

FWHM - Full width at half maxima

TOFMS - Time of flight mass spectroscopy

AFM - Atomic force microscopy

PPA - Pseudopotential simulation

TB - Tight binding model

EL - Electroluminescence

Bibliography

[1] H . Nalwa ,Nanostructured Materials and Nanotechnology, **4** Academic Press (2000).

[2] H . Koyama and N. Koshida, J. Appl. Phys. **74**, 6365 (1993).

[3] J. Cai and C.T. Sah, J. Appl. Phys. **89**, 2272 (2001).

[4] Materials Research Society Bulletin, Special Focus on Emerging Methods of Micro- and Nanofabrication, Academic Press, (2001).

[5] http:// WWW.allianzgroup.com (Accessed in January 2009).

[6] S. K. Ghoshal, Devendra Mohan, Tadesse Tenaw Kassa and Sunita Sharma, Int. J. Mod. Phys. B **21**, 3783 (2007).

[7] P. D. J. Calcott, K . J. Nash , L . T. Canham , M. J.Kane and D.Brumhead, J. Phys. **81**, (1993).

[8] K. E .Andersen, C . Y .Fong and W. E .Pickett , J. Nano. Crys. Solids. **64**, (2000).

[9] http:// WWW.ct.infn.it/matis (Accessed in February 2009).

[10] A . P. Alivisatos , J. Phys. Chem. **100**, 13226 (1996).

[11] M . L . Ciurea, I . Stavarache and V. Iancu , J. Nano. Crys. Solids. **15**, 1802 (2004).

[12] http:// WWW.nanohub.org/nanomaterials (Accessed in March 2009).

[13] Tae-Youb Kim, Nae-Man Park, Kyung-Hyun Kim, Young-Woo Ok, Tae-Yeon Seong, Cheo- Jong Choi and Gun Yong Sung, Mat. Res. Soc. Symp. Proc. **78**, (2004).

[14] P . K Basu, theory of optical processes in semiconductors; Bulk and micro structures, oxford university press, oxford England (1997).

[15] http://www.me.berkeley.edu/nti/englander1.ppt (Accessed in March 2009).

[16] L . Pavesi and Guardini, Brazilian Jornal of Physics **26**,(1996).

[17] http://WWW.nanohub.org/quantum wires (Accessed in Aprile 2009).

[18] C . N . R. Rao, A . Muller and A . K . Cheetham, The Chemistry of Nanomaterials: Synthesis, Properties and Applications. **2** WILEY (2001).

[19] L . T . Canham, Appl. Phys. Lett. **57**, 1046 (1990).

[20] A . L . Erros, M . Rosen, M . Kenvo, M . Nirmal, D . J . norris and M . Bawendi, Phys. Rev. B **54**,4843(1996).

[21] M . V .Wolkin, J . Jorne, PM . Fauchet, G . Allan and C . Delerue. Phys. Lett. **83**,(1999).

[22] Yit-Tsongchen Tamkang, Jo . Sc . and Engg , Appl. Phys. **5**, 99 (2002).

[23] S. F. Li and X. G. Gong, J. Chem . Phys. **122**, 174311 (2005).

[24] P . C . Searson, J . M . Maculay and F . M . Ross, J . Appl. Phys. **72**, (1992).

[25] S . L . Zang, S . P . Wong, I . H . Wilson, S . K . Hardk, Z . F. Liu and S.M. Cai. Appl. Phys. Lett. **69**, (1996).

[26] K . D . Hirschman, L . Tsybeskov, S . P . Duttagupta and F . M. Fauchet. Nature **384**, (2004).

[27] http://en.wikiapedia.org/wiki/porous (Accessed in January 2009).

[28] L . Pavesi and R . Guardini, Brazilian Journal of physics, **26**,(1996).

[29] M . Voos , Ph . Uzan , C . Delalande, G . bastard and A . Hallimaoui, Appl . Phys . Lett . **61**, 1213 (1992).

[30] G . C . John and V . A . Singh, Phys . Rev. B **50** , 5329 (1994).

[31] G . Ledoux, O . Guillois, D . Porterat, and C. Reynaud, Phys. Rev. B **62**, 15954 (2000).

[32] Y . H. xie,M . s. Hybertsen and William L. Wilson, Phys. Rev. B **49** , 5386 (1994).

[33] S. K .Ghoshal, K . P. Jain and R. J .Elliott, J. Metastable and Nano . Cry. Solids. **23**, 7383 (2005).

DECLARATION

I here by declare that this thesis has been presented with the help of my advisor as well as my instructor. All sources of material used for the thesis have been duly acknowledged.

Name: Zebib Yenus

Signature: .....

Place and time of submission: Addis Ababa University, June 2009

This thesis has been submitted for examination with my approval as University advisor.

Name: Dr. Sib. Krishna. Ghoshal

Signature: .....

Addis Ababa University

Department of Physics

June, 2009